Cite this: DOI: 10.1039/c0xx00000x

www.rsc.org/xxxxxx

ARTICLE TYPE

Electrocodeposition of silver and silicomolybdate hybrid nanocomposite for nonenzymatic hydrogen peroxide sensor

Kuo Chiang Lin, Tsung Han Wu and Shen Ming Chen*

Received (in XXX, XXX) Xth XXXXXXXXX 20XX, Accepted Xth XXXXXXXXX 20XX

DOI: 10.1039/b000000x

Novel silver and silicomolybdate (SiMO) hybrid nanocomposite (Ag/SiMO) has been successfully fabricated for nonenzymatic hydrogen peroxide (H_2O_2) detection. The composite is prepared by the electrocodeposition of silver and silicomolybdate and studied by scanning electron microscopy (SEM) and atomic force microscopy (AFM). In neutral condition, the electrode shows good activity towards H_2O_2 reduction with low overpotential. Amperometric response ($E_{app.}$ = -0.2 V) provides linear range of 5×10^{-5}—2.345×10^{-2} M with sensitivity of 974.2 μA mM^{-1} cm^{-2}, detection limit of 1×10^{-7} M (S/N = 3), and response time of 5 s. The Ag/SiMO electrode can analyse H_2O_2 promising a nonenzymatic H_2O_2 sensor due to its low overpotential, high sensitivity, good stability, fast response, and low cost.

1. Introduction

H_2O_2 is one of the most important analytes because H_2O_2 is involved in various fields such as paper bleaching, food processing, textile industry, environmental analysis, cleaning products, minerals processing, oxidative stress study, fuel cell, and reactions of oxidases.[1–5] It also can't be ignored in other fields where H_2O_2 is detected such as study of catalytic effect of particles, biosensors, and medical devices.[6–8] It is of great sense to monitor H_2O_2 accurately and rapidly driven by not only its nature as a side product generated from many enzyme-involved reactions but also its important role as a signaling molecule in regulating various biological processes.[2] Developing the techniques of H_2O_2 determination is, therefore, important.

Electrochemical amperometry technique is found to be an excellent tool for the determination of H_2O_2,[9] as other methods such as chemiluminescence,[10] titrimetry,[11] photometry,[12] and high performance liquid chromatography[13] are not capable of detecting trace concentrations of H_2O_2 and suffer from the interference of other biologically active molecules.[14] Furthermore, electrochemical detection of H_2O_2 has its advantages over other techniques due to its convenience, sensitivity, selectivity, and immediate response. Electrochemical sensors for H_2O_2 determination are basically classified into two major types: enzymatic and nonenzymatic modified sensors. Generally, nonenzymatic biosensors[15-18] make more beneficial with several advantages like stability, simplicity, reproducibility, reusability and cost reduction. Therefore, the development of nonenzymatic sensors has become a trend. Among the enzyme-free sensors, nano-based sensors have been developed.

Recently, graphene or MWCNT composites with Ag, Pt, Au, and Ce nanoparticles have been used in sensor applications.[19–24] Among these materials, silver nanoparticles (AgNPs) demonstrated excellent catalytic activity in sensor fields.[25] The sensor performance of composites could be affected by the shape, size, and dispersion of metal particles on them.[26] Therefore, the composite matrix plays an important role in gaining high dispersion of AgNPs, as well as its respective size and shape. Other reported methods to produce AgNPs–MWCNT composite including templates, chemical reagents, irradiations,[27,28] electrodeposition method,[29] and synthesis by MWCNT without the addition of any chemical (reducing agent) or exposure to irradiation. The AgNPs were reduced to MWCNT surface, causing a good dispersion of AgNPs in the AgNPs–MWCNT composite and displayed good performance toward sensing H_2O_2 at high sensitivity levels.[30,31]

Silicomolybdate (SiMO) polyoxometalate, $SiMo_{12}O_{40}{}^{4-}$, form nanometer-sized polyoxometalate clusters that are of interest in bioanalysis, material science, catalysis, magnetism, surface chemistry and medicine. The polyoxometalate anion is a mixed-valence species and polyoxometalate modified electrodes and their electrocatalytic properties are very important and are the subject of intensive research. Recently, a simple procedure is also proposed for immobilization of copper complex $[Cu(bpy)_2]Br_2$ with silicomolybdate and single-walled carbon nanotubes, presenting a very low detection limit for H_2O_2.[32] The negatively charged silicomolybdate might provide a good chance to coimmobilized with other positively charged and electroactive materials such as silvers.

In the present study, we present a simple and facile one-step method to prepare a silver/silicomolybdate (Ag/SiMO) hybrid nanocomposite for nonenzymatic H_2O_2 sensor. The most notable aspect of our study is the use of the negatively charged silicomolybdate to induce silver co-deposit on electrode surface in an aqueous solution. The hybrid formation of nanometer-sized silver nanoparticles covered on silicomolybdate balls is studied in an aqueous solution without harsh chemicals such as hydrazine during the process. The electrocatalytic property of the hybrid nanocomposite is investigated for electrocatalytic reduction of H_2O_2. All test results are also analyzed regarding to sensitivity, linear range and selectivity toward H_2O_2 detection.

2. Experimental

2.1 Materials and apparatus

Hydrogen peroxide (H_2O_2) and silicomolybdate (SiMO) were purchased from Sigma-Aldrich (USA) and used as received. All other chemicals (Merck) used were of analytical grade (99%). Double-distilled deionized water (> 18.1 MΩ cm^{-1}) was used to prepare all the solutions. All other reagents were of analytical grade and used without further purification.

The Ag/SiMO hybrid composite was characterised by cyclic voltammetry and scanning electron microscopy (SEM). The electrochemical experiments were conducted using a CHI 1205a electrochemical workstation (CH Instruments, USA) with a conventional three-electrode setup using the Ag/SiMO/GCE as the working electrode, an Ag/AgCl (3 M KCl) reference electrode, and a platinum wire counter electrode. A BAS (Bioanalytical Systems, Inc., USA) glassy carbon electrode (GCE) with a diameter of 0.3 cm was used for all electrochemical experiments. All potentials reported in this paper were referred to a Ag/AgCl electrode. The buffer solution was completely deaerated using a nitrogen gas atmosphere. The electrochemical cells were kept properly sealed to avoid interference with oxygen from the atmosphere. In the initial checking for voltammetric signals of all modified electrodes, the signals were confirmed with stability due to no change during 5 scan cycles in the blank solution. Therefore, the voltammograms of different modified electrodes were recorded and presented with the first scan cycle in this work. The composite was analysed by energy dispersive spectroscopy (EDS), and its morphology was characterised by means of SEM and AFM images were recorded with multimode scanning probe microscope. Indium tin oxide (ITO) was used as the substrate for various films in the EDS and SEM analyses.

2.2 Fabrication of the Ag, SiMO, and Ag/SiMO modified electrodes

GCE and ITO substrates were coated with different composites, including Ag, SiMO, and Ag/SiMO, for study in this work.

The Ag modified electrodes were individually prepared in a nitric solution (pH 1.5) containing 4×10^{-2} M $AgNO_3$ using a bare electrode. By consecutive cyclic voltammetry, they were controlled in the potential range of -0.2–1.4 V with a scan rate of 0.1 Vs^{-1} and 20 scan cycles.

The SiMO modified electrodes were prepared by drop-casting. 10 µl of a nitric solution (pH 1.5) containing 1×10^{-3} M silicomolybdate was directly dropped on a bare electrode. The electrodes were further dried out in an oven at 40 ºC.

The electrocodeposition of silver and silicomolybdate was easily carried out in a nitric solution (pH 1.5) containing 4×10^{-2} M $AgNO_3$ and 1×10^{-3} M silicomolybdate using a bare electrode to prepare the Ag/SiMO modified electrode. By consecutive cyclic voltammetry, it was controlled in the potential range of -0.2–1.4 V with a scan rate of 0.1 Vs^{-1} and 20 scan cycles.

Hereafter, the aforementioned processes were used to prepare the Ag, SiMO, and Ag/SiMO, respectively. The modified electrodes were stored at room temperature before use. All modified electrodes were mentioned according to their preparation processes in this work.

3. Results and discussion

3.1 Preparation and characterisation of the Ag/SiMO hybrid composite

Fig. 1 shows the voltammograms of a GCE electrode examined in pH 1.5 nitric solution containing $AgNO_3$ and silicomolybdate. In the first scan cycle, there are three redox couples (redox couple 1, 2, and 3) revealing to $H_4SiMo_{12}O_{40}/H_6SiMo_{12}O_{40}$, $H_6SiMo_{12}O_{40}/H_8SiMo_{12}O_{40}$, and $H_8SiMo_{12}O_{40}/H_{10}SiMo_{12}O_{40}$ redox processes.[33] The redox couple 4 can be recognized as Ag(0)/Ag(I) redox process.[30] It can be seen that redox peak currents increase with the increase of scan cycle. In particular, the redox couple 4 has strong current development. This result implies that the silicomolybdate is covered or wrapped by silver. In the formation process, the negatively charged silicomolybdate is attracted to positively silver ions to form the Ag/SiMO hybrid composite and deposit on electrode surface.

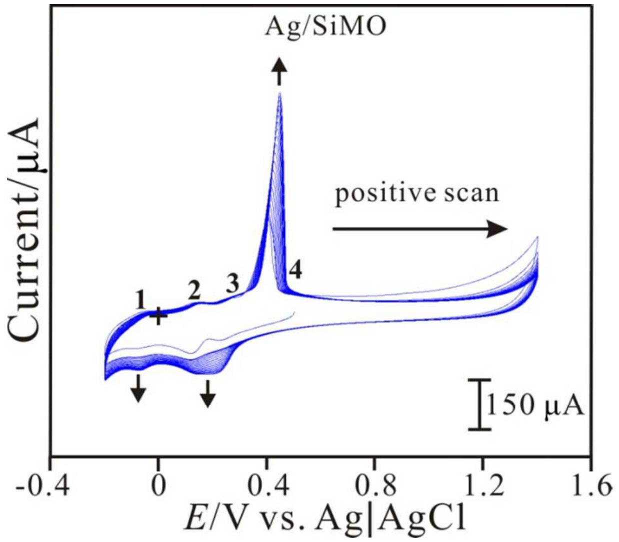

Fig. 1 Consecutive cyclic voltammograms of a glassy carbon electrode examined in nitric solution (pH 1.5) containing 4×10^{-2} M $AgNO_3$ and 1×10^{-3} M silicomolybdate. Scan rate = 0.1 Vs^{-1}. Scan cycle = 20.

Fig. 2A-C shows the SEM images for (A) Ag, (B) SiMO, and (C) Ag/SiMO, respectively. Fig. 2A-C exhibit clusters, porous flat sheets, and dendritic structures for (A) Ag, (B) SiMO, and (C) Ag/SiMO, respectively. The specific dendritic image is different from the Ag (Fig. 2A) and SiMO (Fig. 2B). This result indicates that the Ag/SiMO can be successfully immobilized on electrode surface due to the hybrid formation of Ag and SiMO. The specific dendritic structure of Ag/SiMO was further characterized by EDS (Fig. 2D). 100% of Ag is checked by the test report. The result indicates that the silicomolybdate might be wrapped by a lot of silver atoms. This phenomenon also indicates that one silicomolybdate molecule can collect a lot of silver atoms to codeposit on electrode surface. One can conclude that the specific dendritic Ag/SiMO can be performed through this artwork.

Fig. 3 shows the AFM images for (A) Ag, (B) SiMO, and (C) Ag/SiMO, respectively. The AFM images of these modifiers show average particle size of 32.0 nm, 56.2 nm, and 39.8 nm for Ag, SiMO, and Ag/SiMO, respectively. These modifiers are also proved in nanocomposites with average roughness of 16.7 nm, 11.6 nm, and 31.7 nm, respectively. The Ag/SiMO shows specific cluster nanostructure indicating that Ag and SiMO hybrid nanoparticles can be easily immobilized on electrode surface. They display similar morphological properties in the results of SEM and AFM. One can conclude that the hybrid nanocomposite (Ag/SiMO) can be easily prepared by the method.

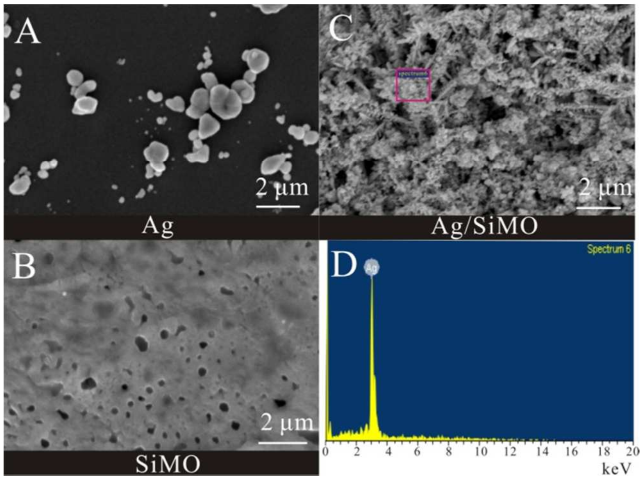

Fig. 2 SEM images of (A) Ag, (B) SiMO, and (C) Ag/SiMO coated ITO electrodes. (D) EDS spectrum of the Ag/SiMO for the SEM image (C).

Different materials modified electrodes were prepared and studied by cyclic voltammetry. Fig. 4A shows the voltammograms of (a) Ag, (b) SiMO, and (c) Ag/SiMO modified electrodes. The modified electrodes shows significant redox peaks while bare electrode (curve (d)) shows no redox peaks. As the scale-up voltammograms shown in Fig. 4B, the Ag modified electrode (curve (a)) shows only one obvious redox couple with formal potential ($E^{0'}$) of +0.295 V (E_{pa} = +0.491 V, E_{pc} = +0.099 V) reveals to the redox process of Ag(0)/Ag(I) while the SiMO (curve (b)) shows three redox couples with formal potential of $E^{0'}_1$ = -0.215 V, $E^{0'}_2$ = +0.069 V, $E^{0'}_3$ = +0.282 V for redox processes of $H_4SiMo_{12}O_{40}$/$H_6SiMo_{12}O_{40}$, $H_6SiMo_{12}O_{40}$/$H_8SiMo_{12}O_{40}$, and $H_8SiMo_{12}O_{40}$/$H_{10}SiMo_{12}O_{40}$, respectively.

Particularly, the Ag/SiMO shows the specific redox couple different from both Ag and SiMO modified electrodes. It shows only one redox couple ($E^{0'}$ = +0.345 V; E_{pa} = +0.688 V, E_{pc} = +0.002 V) which is more positive than that of the Ag modified electrode. The formal potential difference might indicate that the new composite is formed or some special film formation process can be proposed. In this case, the film formation might be explained by that the spherical and negatively charged SiMO induced more Ag deposit on electrode surface. Therefore, the Ag/SiMO shows only one redox couple but higher than that of Ag.

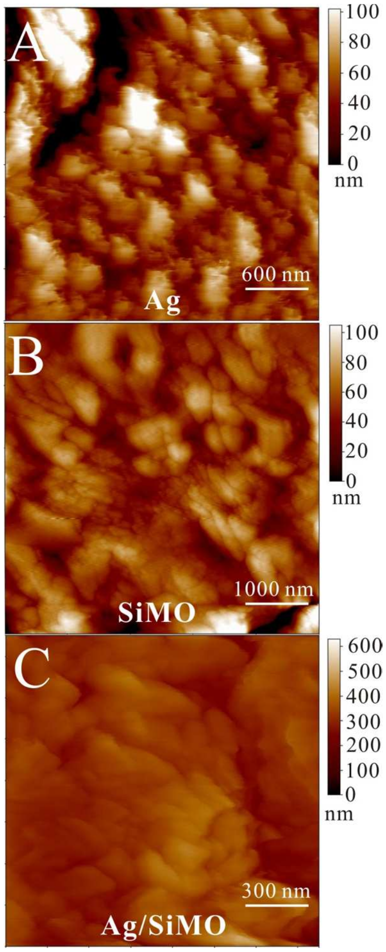

Fig. 3 AFM images of (A) Ag, (B) SiMO, and (C) Ag/SiMO coated ITO electrodes.

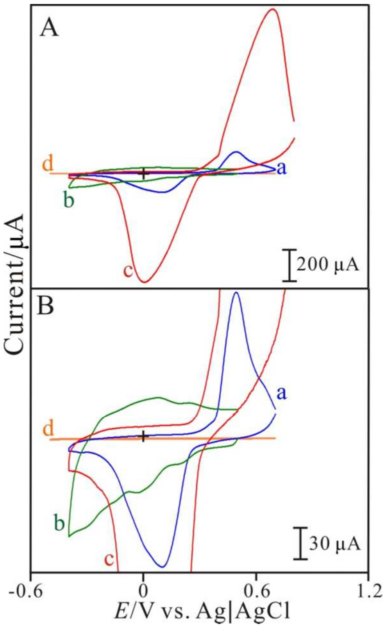

Fig. 4 (A) Cyclic voltammograms of a modified glassy carbon electrode examined in pH 7 PBS with different modifiers including (a) Ag, (b) SiMO, (c) Ag/SiMO, and (d) bare GCE, respectively. Scan rate = 0.1 Vs^{-1}. (B) Scale-up cyclic voltammograms of (A).

The cathodic peaks were integrated to speculate the electrochemical surface area for Ag and Ag/SiMO. The quantity of electricity is evaluated as 94.3 μC and 568.8 μC for Ag and Ag/SiMO, respectively. The Ag/SiMO hybrid nanocomposite shows specific quantity of electricity which is almost six times higher than that of the Ag. One can know that the specific hybrid composite contributes more quantity of electricity resulting from the enhanced surface area.

3.2 Electrocatalytic reduction of H_2O_2 at the Ag/SiMO electrode

The related modified electrodes were prepared to study the electrocatalytic reduction of H_2O_2. Fig. 5 shows the voltammograms of bare and Ag/SiMO modified electrode examined in the absence/presence of H_2O_2. It shows high current response to H_2O_2 concentration. By the comparison between curve (a) and (b), the cathodic peak current of Ag/SiMO increases in the increase of H_2O_2 concentration. It is noticed that the cathodic peak potential is found at -0.16 V. It shows lower overpotential and higher current response to H_2O_2 when compared to that of bare electrode (curve (c)). The reduction potential is corresponding to a redox process for Ag(I)/Ag(0). As indicated in the literature, the reduction of H_2O_2 to H_2O was catalysed by the Ag(I)/Ag(0) redox process according to the following reactions:

$$\text{Ag(I)-composite} + e^{-} \rightarrow \text{Ag(0)-composite} \qquad (1)$$

$$2\text{Ag(0)-composite} + H_2O_2 + 2H^{+} \rightarrow 2\text{Ag(I)-composite} + 2H_2O \qquad (2)$$

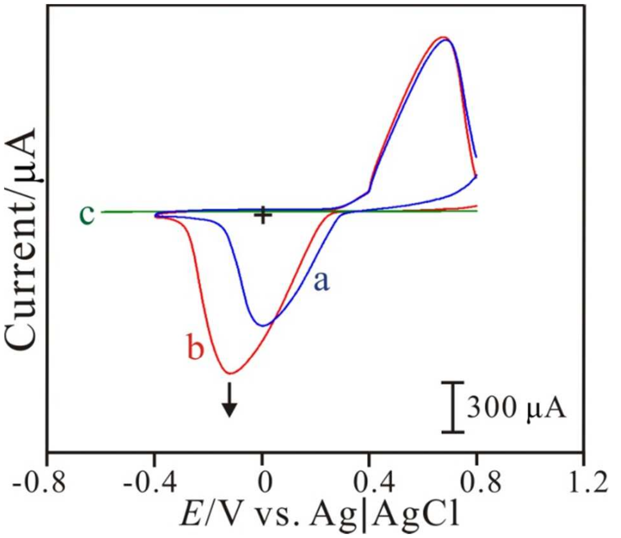

Fig. 5 Cyclic voltammograms of Ag/SiMO modified glassy carbon electrode examined in pH 7 PBS with $[H_2O_2]$ = (a) blank and (b) 1×10^{-4} M, respectively. Scan rate = 0.1 Vs^{-1}. (c) Bare electrode is examined in the presence of 1×10^{-4} M H_2O_2.

3.3 Amperometric response of the Ag/SiMO electrode to H_2O_2

Fig. 6A shows the amperometric response of the Ag/SiMO electrode examined with several additions of H_2O_2 spiked into pH 7 PBS. The response curve turns downward with increasing concentration because an increasing amount of intermediate species is adsorbed onto the electrode surface, prolonging the reaction time. From the inset (a) of Fig. 6A, the detection limit is estimated in 0.1 μM (1×10^{-7} M) based on signal/noise = 3. A fast response time of 5 s is also found in the inset. The calibration curve for nonenzymatic H_2O_2 sensor is shown in the inset (b) of Fig. 6A. The red straight line of the inset (b) represents the linearity with linear concentration range of 5×10^{-5}–2.345×10^{-2} M. It provides the regression equation, $I_{pc}(\mu A) = 69.1C_{H2O2}(mM) + 25.4$, with correlation coefficient of $R^2 = 0.995$. By estimation, the electrode shows sensitivity of 974.2 $\mu A\ mM^{-1}\ cm^{-2}$.

The Ag/SiMO composite was compared with various modifiers for nonenzymatic H_2O_2 sensors in Table 1. It shows competitive performance among these modifiers. Particularly, the Ag/SiMO modified electrode shows high sensitivity to those using Prussian blue, MWCNT, and expensive materials, such as ionic liquid and other noble metal-MWCNT hybrid composite. When compared to some noble metal-based hybrid composites such as Pt, Au, and Ag metals, the Ag/SiMO electrode also shows benefit in low cost by our method. Good performance is clearly disclosed due to the specific Ag/SiMO composite. The hybrid composite significantly increases the electrocatalytic active areas and promotes electron transfer in the reduction of H_2O_2. The Ag/SiMO hybrid composite based electrochemical sensor exhibits high sensitivity and other competitive performance such as low overpotential and wide linear concentration range, suggesting as an ideal electrocatalyst in the literature for nonenzymatic H_2O_2 sensors.

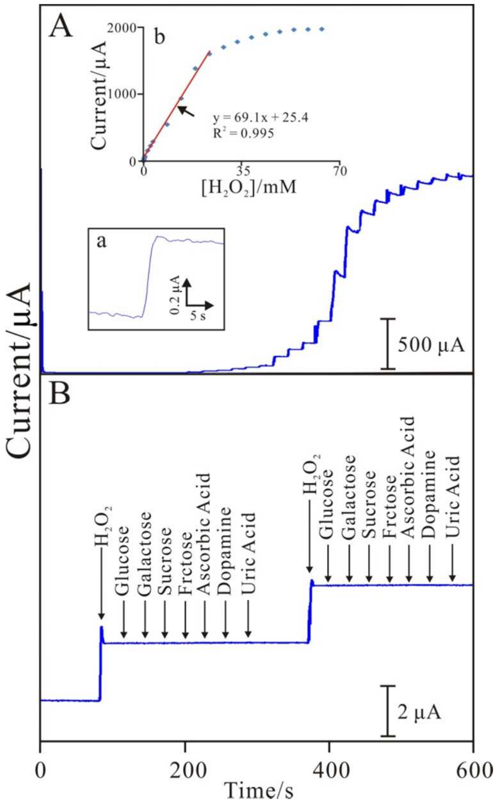

Fig. 6 Amperograms of Ag/SiMO/GCE examined in pH 7 PBS with several additions of (A) H_2O_2 (started from 0.1 μM to 5 mM) and (B) interferents (each for 10^{-5} M). Electrode rotation speed = 2000 rpm. $E_{app.}$ = -0.2 V. Insets: (a) the scale-up amperogram in the presence of 0.1 μM H_2O_2 and (b) the calibration curve.

Table 1 Performance of the Ag/SiMO composite compared with various modifiers for nonenzymatic H_2O_2 sensors.

Modifiers	$E_{app.}$[a] (V vs. Ag/AgCl)	Sensitivity (μA mM^{-1} cm^{-2})	LOD[b] (μM)	Linear range (μM)	Ref.
Graphene–MWCNTs	-0.40	15.2	9.4	20–2100	[34]
Graphene–CS/PB	0.05	816.4	0.21	10–400	[35]
PVP–Ag NWs	-0.30	15.86	2.3	20–3620	[36]
RGO/Fe_3O_4	-0.30	688	3.2	100–6000	[37]
PB/RTIL/CNTs	0.21	185.9	0.49	0.49–700	[38]
Ag-MnO_2-MWCNT	-0.3	82.5	1.7	5–10400	[39]
PtAu/G-CNTs	-0.47	313.4	0.6	2–8561	[40]
Nafion-PB-MWCNTs/SPCE-IL	0	436	0.35	5–1645	[41]
Ag/SiMO	-0.2	974.2	0.1	50–23450	This work

[a] $E_{app.}$ = Applied potential.

[b] LOD = Limit of detection.

3.4 Reproducibility, stability, and anti-interference property of the Ag/SiMO electrode

The reproducibility and stability of the sensor were evaluated. Five Ag/SiMO electrodes were investigated by amperometry ($E_{app.}$ = -0.2 V).

The amperometric responses of the Ag/SiMO/GCE were obtained in pH 7 PBS with sequential additions of 5×10^{-4} M H_2O_2. The relative standard deviation (R.S.D.) was 4.3%, confirming the high reproducibility of the preparation method. Ten successive measurements of H_2O_2 on one Ag/SiMO electrode yielded an R.S.D. of 4.1%, indicating that the sensor was stable. The long-term stability of the sensor was also evaluated by measuring its current response to H_2O_2 within a 7-day period. The sensor was exposed to air, and its sensitivity was tested every day. The current response of the Ag/SiMO electrode was approximately 93% of its original counterpart, which can be mainly attributed to the chemical stability of Ag/SiMO in neutral solution.

Based on these results, the Ag/SiMO electrode shows a nearly constant peak current towards H_2O_2 reduction, indicating that the electrode is very stable in the determination of H_2O_2.

Fig. 6B shows the amperometric response of Ag/SiMO/GCE examined in pH 7 PBS with sequential additions of H_2O_2 and potential interferents including glucose, galactose, sucrose, fructose, ascorbic acid, dopamine, and uric acid (1×10^{-4} M for each addition). A well-defined H_2O_2 response was obtained, and insignificant responses were observed for interfering species. As the results, the Ag/SiMO electrode shows good selectivity for H_2O_2 detection.

4. Conclusions

The Ag/SiMO hybrid nanocomposite can be successfully prepared on electrode surface by a simple method. It shows competitive performance for effective determination of H_2O_2. The novel nonenzymatic H_2O_2 sensor presents attractive features, such as low overpotential, high sensitivity, high selectivity, simple method, low cost, and test in neutral condition.

Acknowledgements

We acknowledge the Ministry of Science and Technology (Project No. 101-2113-M-027 -001 -MY3), Taiwan.

Notes and references

Electroanalysis and Bioelectrochemistry Lab, Department of Chemical Engineering and Biotechnology, National Taipei University of Technology, No.1, Section 3, Chung-Hsiao East Road, Taipei 106, Taiwan (ROC). Fax: (886)-2-27025238; Tel: (886)-2-27017147; E-mail: smchen78@ms15.hinet.net

† Electronic Supplementary Information (ESI) available: [details of any supplementary information available should be included here]. See DOI: 10.1039/b000000x/

‡ Footnotes should appear here. These might include comments relevant to but not central to the matter under discussion, limited experimental and spectral data, and crystallographic data.

1 N.A. Sitnikova, A.V. Borisova, M.A. Komkova and A.A. Karyakin, *Anal. Chem.*, 2011, **83**, 2359.
2 W. Chen, S. Cai, Q.Q. Ren, W. Wen and Y.D. Zhao, *Analyst*, 2012, **137**, 49.
3 A.L. Brioukhanov and A.I. Netrusov, *Appl. Biochem. Microbiol.*, 2007, **4**, 567.
4 F. Alcaide, P.L. Cabot and E. Brillas, *J. Power Sources*, 2006, **153**, 47.
5 S. Fukuzumi, Y. Yamada and K.D. Karlin, *Electrochim. Acta*, 2012, **82**, 493.
6 N.P. Sardesai, D. Andreescu and S. Andreescu, *J. Am. Chem. Soc.*, 2013, **135**, 16770.
7 N.P. Sardesai, A. Karimi and S. Andreescu, *ChemElectroChem*, 2014, **1**, 2082.
8 N.P. Sardesai, M. Ganesana, A. Karimi, J.C. Leiter and S. Andreescu, *Anal. Chem.*, 2015, **87**, 2996.
9 C.Y. Lin, Y.H. Lai, A. Balamurugan, R. Vittal, C.W. Lin and K.C. Ho, *Talanta*, 2010, **82**, 340–347.
10 S. Hanaoka, J.M. Lin and M. Yamada, *Anal. Chim. Acta*, 2001, **426**, 57.
11 E.C. Hurdis and J.H. Romeyn, *Anal. Chem.*, 1954, **26**, 320.
12 A. Saifer and S. Gerstenfeld, *J. Lab. Clin. Med.*, 1958, **51**, 448.
13 U. Pinkernell, S. Effkemann and U. Karst, *Anal. Chem.*, 1997, **69**, 3623.
14 X. Wang, T. Yang, Y. Feng, K. Jiao and G. Li, *Electroanalysis*, 2009, **21**, 819.
15 T. Pirmohamed, J.M. Dowding, S. Singha, B. Wassermana, E. Heckert, A.S. Karakoti, J.E.S. King, S. Seal and W.T. Self, *Chem. Commun.*, 2010, **46**, 2736.

16 A.S. Karakoti, N.A. Monteiro-Riviere, R. Aggarwal, J.P. Davis, R.J. Narayan, W.T. Self, J. McGinnis and S. Seal, *JOM (1989)*, 2008, **60**, 33–37.

17 E.G. Heckert, A.S. Karakoti, S. Seal and W.T. Self, *Biomaterials*, 2008, **29**, 2705.

18 A. Asati, S. Santra, C. Kaittanis, S. Nath and J.M. Perez. *Angew. Chem. Int. Ed.*, 2009, **48**, 2308.

19 L. Feng, G. Gao, P. Huang, X. Wang, C. Zhang, J. Zhang, S. Guo and D. Cui, *Nanoscale Res. Lett.*, 2011, **6**, 1.

20 H. Rajabzade, P. Daneshgar, E. Tazikeh and R.Z. Mehrabian, *J. Chem.*, 2012, **9**, 2540.

21 X. Liu, X. Xu, H. Zhu and X. Yang, *Anal. Methods*, 2013, **5**, 2298.

22 Q. Wang and Y. Yun, *Microchim. Acta*, 2013, **180**, 261.

23 B. Yu, J. Feng, S. Liu and T. Zhang, *RSC Adv.*, 2013, **3**, 14303.

24 C.H. Chen, Y.J. Chiou, W.J. Liou, W.S. Lin, H.M. Lin and S.H. Wu, *Funct. Mater. Lett.*, 2011, **4**, 295.

25 C. Welch, C. Banks, A. Simm and R. Compton, *Anal. Bioanal. Chem.*, 2005, **382**, 12.

26 H. Chen, Z. Zhang, D. Cai, S. Zhang, B. Zhang, J. Tang and Z. Wu, *Talanta*, 2011, **86**, 266.

27 S.S. Bale, P. Asuri, S.S. Karajanagi, J.S. Dordick and R.S. Kane, *Adv. Mater.*, 2007, **19**, 3167.

28 J. Lin, C. He, Y. Zhao and S. Zhang, *Sens. Actuators B*, 2009, **137**, 768.

29 Y.C. Tsai, P.C. Hsu, Y.W. Lin and T.M. Wu, *Electrochem. Commun.*, 2009, **11**, 542.

30 W. Zhao, H. Wang, X. Qin, X. Wang, Z. Zhao, Z. Miao, L. Chen, M. Shan, Y. Fang and Q. Chen, *Talanta*, 2009, **80**, 1029.

31 X. Li, Y. Liu, L. Zheng, M. Dong, Z. Xue, X. Lu and X. Liu, *Electrochim. Acta*, 2013, 113, 170.

32 A. Salimi, A. Korani, R. Hallaj, R. Khoshnavazi and H. Hadadzadeh, *Anal. Chim. Acta*, 2009, **635**, 63.

33 Y.T. Chang, K.C. Lin and S.M. Chen, *Electrochim. Acta*, 2005, **51**, 450.

34 S Woo, Y. R. Kim, T.D. Chung, Y. Piao and H. Kim, *Electrochim. Acta,* 2012, **59**, 509.

35 J.H. Yang, N. Myoung and H.G. Hong, *Electrochim. Acta*, 2012, **81**, 37.

36 X. Yang, J. Bai, Y.Wang, X. Jiang and X. He, *Analyst*, 2012, **137**, 4362.

37 Y. Ye, T. Kong, X. Yu, Y. Wu, K. Zhang and X. Wang, *Talanta*, 2012, **89**, 417.

38 A.H. Keihan and S. Sajjadi, *Electrochim. Acta*, 2013, **113**, 803.

39 Y. Han, J.B. Zheng and S.Y. Dong, *Electrochim. Acta*, 2013, **90**, 35.

40 D.B. Lu, Y. Zhang, S.X. Lin, L.T. Wang and C.M. Wang, *Talanta*, 2013, **112**, 111.

41 X. Zhu, X. Niu, H. Zhao and M. Lan, *Sens. Actuator B*, 2014, **195**, 274.

42